DOI: 10.1002/ejic.201001039

Dinuclear Ru–Cu Complexes: Electronic Characterisation and Application to Dye-Sensitised Solar Cells

Keri L. McCall,[a] James R. Jennings,[b] Hongxia Wang,[b] Ana Morandeira,[c] Laurence M. Peter,[b] James R. Durrant,[c] Lesley J. Yellowlees,[a] and Neil Robertson*[a]

Keywords: Ruthenium / Copper / Dinuclear complexes / Dye-sensitized solar cells / Supramolecular chemistry

We prepared the complexes [Ru{4,4′-(CO_2R-bpy)$_2$}{Cu(*exo*O_2-cyclam)}][NO_3]$_2$ [R = Et (**1**), H (**2**)], which possess a Cu^{II} centre covalently linked to a (bipyridyl)Ru^{II} fragment. The complexes were characterised by cyclic voltammetry, UV/Vis spectroscopy, hybrid DFT and TD-DFT (time-dependent density-functional theory) calculations, EPR (electron paramagnetic resonance), emission spectroscopy and UV/Vis spectroelectrochemistry, with the latter showing reversible conversion to the mono- and di-oxidised and mono- and di-reduced species. The data suggest the first oxidation to be largely based on the Ru centre but with little energetic difference between the highest occupied orbitals based on Ru and based on Cu. There was also evidence of solvent coordination in both the electrochemistry and spectroelectrochemistry experiments. The redox potentials and the strong visible absorptions of **2** (λ_{max} = 562 nm, ε_{max} = 22200 $M^{-1}cm^{-1}$) make it appropriate for study as a sensitiser in a dye-sensitised solar cell. Charge-separated lifetime of photoexcited **2** on TiO_2 and incident photon-to-current conversion efficiency (IPCE) as a function of wavelength were studied and are discussed alongside the formation of dye-sensitised solar cells with the best efficiency achieved of η = 2.55 %, V_{oc} = 608 mV, I_{sc} = 5.84 mA cm^{-2} and *ff* = 0.72. Limitations to the maximum efficiency obtained were attributed to a mismatch between the bipyridyl-based unoccupied orbital of the dye and the TiO_2 conduction band edge.

Introduction

Dye-sensitised solar cells (DSSC) have emerged as an important developing technology for low-cost solar energy conversion and a crucial element of these devices is the dye, responsible for light harvesting and control of interfacial electron-transfer processes.[1] A number of examples of dye exist in the literature, which link a (polypyridyl)ruthenium complex to another platinum group metal complex such as Ru^{II}, Os^{II}, Re^{I} or Rh^{III} by a bridging ligand.[2–6] These systems are often referred to as heterosupramolecular triads when adsorbed on the surface of TiO_2 as the semiconductor becomes an active component in the system. A number of problems can arise with these types of sensitisers, for example if a flexible linker [e.g. bis(pyridyl)ethane] is used to couple the two complexes it can be hard to control the orientation of the whole dye. This may lead to the resultant dye cation hole being closer to the surface than desired, and hence the long-lived charge-separated state is not achieved. In addition the size of these dyes may be much larger than that of a mononuclear complex and can lead to poor pore filling on the TiO_2 and lower dye coverage, leading to a lower efficiency cell.[7] Despite these issues, efficient charge separation has been achieved with polynuclear complexes, and a long-lived state on the millisecond timescale has been observed for a trinuclear ruthenium complex.[8]

We have previously investigated Cu(*exo*O_2-cyclam) as a redox-active ligand for first-row transition metals and a (bipyridyl)Ru fragment.[9–11] In these studies the Cu(*exo*O_2-cyclam) ligand was found to exhibit electronic communication between metal centres in trinuclear copper, cobalt, nickel, iron and manganese complexes. Numerous studies have also been carried out by other groups, particularly Tang et al., incorporating this ligand into other heteropolynuclear complexes containing a wide range of first-row transition metals and lanthanides, yielding interesting magnetic properties.[12–18] In this report, we extend this approach to prepare dinuclear Cu–Ru complexes with acid- and ester-substituted (bipyridyl)Ru fragments, with the former suitable for binding to TiO_2, and investigate application to dye-sensitised solar cells. This has allowed investigation of dinuclear complexes that are smaller than the typical dinuclear systems containing two platinum group metal complexes. The general formula of the complexes synthesised is [Ru{4,4′-(CO_2R-bpy)$_2$}{Cu(*exo*O_2-cyclam)}][NO_3]$_2$ (R = Et and H)

[a] School of Chemistry and EaStChem, University of Edinburgh, King's Buildings, Edinburgh, UK
Fax: +44-131-6504743
E-mail: neil.robertson@ed.ac.uk
[b] Department of Chemistry, University of Bath, Bath, BA2 7AY, UK
[c] Centre for Electronic Materials and Devices, Department of Chemistry, Imperial College London, London, SW7 2AZ, UK
Supporting information for this article is available on the WWW under http://dx.doi.org/10.1002/ejic.201001039.

(Figure 1). The ester analogue aids electronic characterisation of the system due to greater solubility, whereas the acid analogue was used for binding to TiO_2.

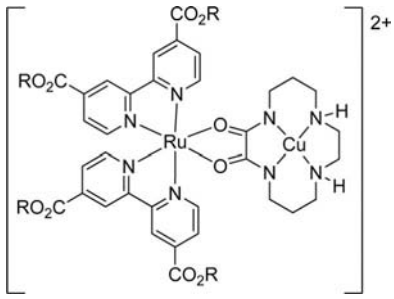

Figure 1. Structure of complexes **1** (R = Et) and **2** (R = H).

There are no existing DSSC studies with (polypyridyl)-ruthenium moieties covalently attached to a copper complex. There are, however, several biological, sensor and electrochromic studies utilising complexes with both a ruthenium and copper moiety where the complexes have been fully characterised, showing evidence of communication between the ruthenium and copper centres.[19–26]

Results and Discussion

Synthesis of complexes **1** and **2** was achieved by reaction of $[Ru(decbpy)_2Cl_2]$ (decbpy = 4,4′-CO_2Et-2,2′-bipyridyl) with $AgNO_3$ to remove chlorido ligands followed by treatment with solid Cu(*exo*O_2-cyclam). Preparation of complex **2** included an additional base hydrolysis step before adding the Cu^{II} species to form the acid substituents.

The electrochemistry of **1** in dimethylformamide (DMF) (Figure 2, Table 1) was found to exhibit unusual behaviour with respect to the oxidations. At slow scan rates there appear to be three distinct oxidations, with the first and third processes becoming more and less defined, respectively, with increasing scan rate. Further investigation of the electrochemistry at –40 °C (Figure S1) still showed the presence of three oxidations; however, there was very little change in the definition of the peaks with varying scan rate at this temperature. The reversibility of the first oxidation is also increased upon reducing the temperature suggesting that the rate constant for the decomposition of the oxidised species becomes smaller as the temperature is lowered. The second and third oxidations remain irreversible at low temperature.

Table 1. Redox potentials of **1**, **2** and related species carried out in 0.1 M $TBABF_4$/DMF (vs. Ag/AgCl) at room temperature.

	$E_{1/2}^{ox}$ [V]			$E_{1/2}^{red}$ [V]		
Cu[a]		0.17				
CuRu[b]	1.60[c]	0.76	–1.15[c]	–1.41	–1.70[c]	
1	1.39[c]	1.17	–0.92	–1.13	–1.25	–1.70[c]
2	1.25[c]	1.04[c]	–0.93[c]	–1.21[c]	–1.63[c]	

[a] Cu(*exo*O_2-cyclam).[10] [b] $[(bpy)_2Ru\{Cu(exoO_2\text{-cyclam})\}](NO_3)_2$.[11] [c] Irreversible.

To investigate if these phenomena were solvent-dependent, the electrochemistry of **1** was also studied in dichloromethane (DCM) (Figure S2). In this noncoordinating solvent the cyclic voltammetry (CV) (and differential pulse voltammogram) showed only two oxidations, the first reversible and the second irreversible. This is very strong evidence for solvent coordination playing a role upon oxidation of the complex. In the strongly coordinating solvent DMF, upon mono-oxidation of the dye, a second oxidation very close in potential is observed, which is also seen to be less dominant with increasing reversibility of the first oxidation, i.e. at lower temperature and faster scan rates. The fact that this second oxidation is not observed in DCM and that the first oxidation is seen to be fully reversible is consistent with solvent coordination in DMF upon oxidation. In addition, our previous report of the crystal structure of the corresponding complex without ester groups[11] showed the complex crystallised with two nitrate counter anions in the axial positions above and below the copper atom. It is reasonable to assume that solvent molecules could occupy these positions if the solvent is highly coordinating.

The reductions seen for **1** (Figure 3, Table 1) were slightly more positive than typical for analogous $[Ru(decbpy)_2X_2]$ complexes.[27] Assuming the first reduction to be that of the singly occupied molecular orbital (SOMO), which is presumably metal-based, this observation is not unexpected.

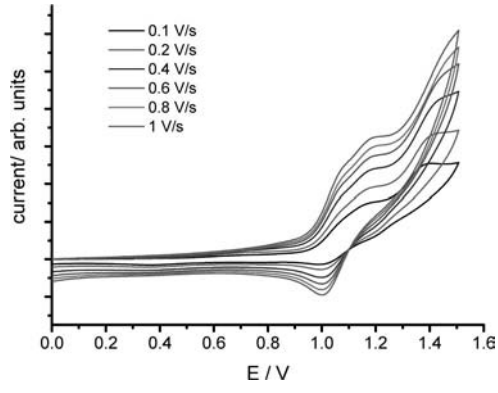

Figure 2. Oxidative CV studies of **1** in 0.1 M $TBABF_4$/DMF at room temperature.

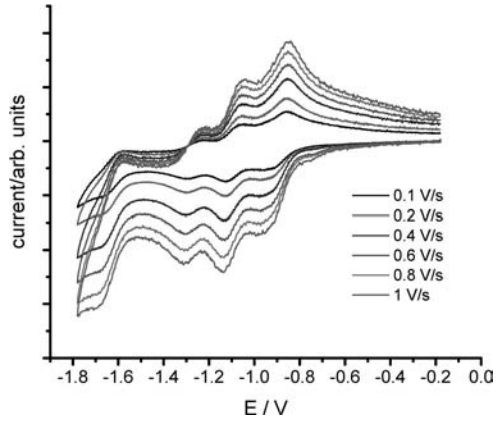

Figure 3. Reductive CV study of **1** in 0.1 M $TBABF_4$/DMF at room temperature.

The second and third reductions are more similar to the reduction potentials of the bipyridyl ligands seen for related systems.[27]

The electrochemistry of Cu(*exo*O_2-cyclam) has been studied previously and was found to have one reversible oxidation at +0.17 V (vs. Ag/AgCl). However, in a trinuclear complex $[Cu\{Cu(exoO_2\text{-cyclam})\}_2]^{2+}$ the macrocycle oxidation process was found to shift to the more positive potential of +0.5 V (vs. Ag/AgCl).[10] The shift from free ligand to complex was thought to be the result of an increased positive charge density from the central Cu^{II} ion. In keeping with this, oxidation of the Cu(*exo*O_2-cyclam) in these ruthenium complexes, whether it be the first or second oxidation, has also shifted to a more positive potential.

For **1** and **2**, two visible bands and one UV band were observed in DMF (Figure 4, Table 2), with the visible bands assigned as having charge-transfer character (vide infra). The energy of the absorption bands for **2** are lower, and the molar extinction coefficients significantly higher than for that of N719.[28] This is in keeping with previous work showing that O-donor ligands, such as acetylacetonato, can be successfully employed to yield lower energy absorption maxima.[29] These properties can be advantageous when fabricating DSSCs as less dye will be required to yield comparable light harvesting efficiency, when comparing to N719 for example, and hence thinner cells can be made. These thinner cells can lead to decreased charge carrier recombination particularly in solid-state cells. The lower energy bands suggest that the use of the O-donor groups has resulted in a destabilisation of the Ru t_{2g} orbitals resulting in a smaller HOMO–LUMO transition and an increased absorption range.

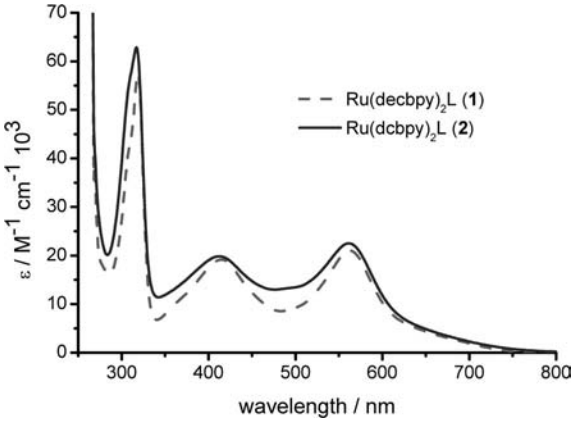

Figure 4. Absorption spectra of **1** and **2** in DMF.

Emission studies were carried out in ethanol at room temperature and 77 K for **1** and **2** (Figure S3). No emission was observed at room temperature, even after degassing of the solution; however, weak emission was observed for **1** and **2** at 77 K with maxima at 760 and 740 nm, respectively. The excitation and emission spectra for both complexes show a large pseudo-Stokes shift indicating emission from a ^{3}MLCT state. The excitation spectra closely resemble the absorption spectra for each of the complexes, confirming that these transitions originate from **1** and **2**. The low emission intensity for **1** and **2** is untypical of such (bipyridyl)Ru complexes and may result from the emission from the ^{3}MLCT excited state being largely quenched due to either intramolecular electron transfer (eT) from the Cu^{II} centre or energy transfer (ET) to excitations based on the copper ligand.

Table 2. Wavelength of transitions and molar extinction coefficients for **1** and **2** in DMF.

Complex	π–π* [nm][a]	MLCT [nm][a]	
CuRu[b]	297 (65.9)	530 (10.1)	365 (11.3)
1	319 (61.4)	561 (21.0)	415 (19.1)
2	317 (64.2)	562 (22.2)	413 (19.6)

[a] Molar extinction coefficient [10^3 M^{-1} cm^{-1}] in parentheses. [b] $[(bpy)_2Ru\{Cu(exoO_2\text{-cyclam})\}](NO_3)_2$.[11]

As mentioned in the Introduction, a number of polynuclear systems have been synthesised and characterised that contain a (polypyridyl)ruthenium moiety covalently attached to a copper system. In a number of these studies the emission of the (polypyridyl)ruthenium moiety was not preserved upon binding of copper(II), which was attributed as above to either eT or ET to/from the copper(II) atom. In the former case the formation of an Ru^{III}–Cu^{I} or Ru^{I}–Cu^{III} transient species could occur. For the systems studied previously this possibility has been ruled out largely due to the Cu^{I}/Cu^{II} couple being very negative with respect to the Ru^{II}/Ru^{III} couple. This is likely to be the case for complexes **1** and **2** also, as the Cu^{I}/Cu^{II} occurs at approximately –1 V (vs. Ag/AgCl) compared to an Ru^{II}/Ru^{III} potential of >0.7 V. However, in contrast to the studies in the literature, the possibility of electron transfer from the Cu^{II} to the excited Ru^{II} centre may potentially occur in the present system. The possibility of a secondary electron transfer from Cu^{II} to oxidised Ru^{III} is very relevant to enhanced charge separation following electron transfer to TiO_2 and is discussed further below.

Spectroelectrochemical studies of **1** were carried out by using an optically transparent thin-layer electrode (OTTLE) in both 0.1 M $TBABF_4$/DMF and 0.3 M $TBABF_4$/DCM to explore the nature of the frontier orbitals and also to give insight into the possibility of solvent coordination in DMF. The mono-oxidation of **1** in DMF showed collapse of the CT bands and a broadening of the intraligand band (Figure S4). The study in DMF was, however, found to be only partially reversible with the regenerated spectrum being very similar to the original dicationic spectrum, yet slightly shifted to a higher energy and with a lower intensity. This may be indicative of the fact that the solvent coordination is not destructive {as is the case for other dye series studied; cf. $[Ru(decbpy)_2](NCS)_2$ for example}[30] but is instead coordinating in the axial positions above and/or below the copper(II).

In order to draw more detailed conclusions about the oxidised species of this complex, the OTTLE studies were also carried out in 0.3 M $TBABF_4$/DCM. Mono-oxidation showed the same observations as in the DMF study with

the collapse of the CT bands and broadening of the intraligand band (Figure S5, Table S1). This study was fully reversible back to the original spectrum upon reversal of the applied potential to 0 V, showing no evidence of solvent coordination, as expected from the electrochemistry studies. The changes in the spectrum upon mono-oxidation are consistent with oxidation of the Ru^{II} centre to Ru^{III}.[27] Di-oxidation (Figure S5) showed only minor additional changes, with the growth of a small band at 27000 cm^{-1} and an increase in the second intraligand band at 30000 cm^{-1}. The di-oxidised study was also found to be reversible. The lack of any further changes to the MLCT bands of the (bipyridyl)Ru framework is consistent with the second oxidation being largely of Cu^{II}/Cu^{III} character.

The reductive OTTLE studies of **1** (Table S1) were carried out in 0.1 M $TBABF_4$/DMF. The mono-reduction (Figure 5) showed a decrease in intensity and slight shift to lower energy of the MLCT bands and a broadening of the bipyridyl intraligand band. This indicates that the initial reduction is not a bipyridyl-based orbital process as in a typical (bipyridyl)ruthenium complex,[27,31] suggesting it is instead a reduction of the Cu^{II} centre. This observation also agrees with the reductive electrochemistry study where the first reduction occurred at a less negative potential than would be expected for a bipyridyl ligand and hence can be assigned as a copper-based reduction. The di-reduced study (Figure S6) on the other hand showed typical changes in absorption that would be expected for a bipyridyl-based reduction. This includes the decrease in intensity of the band at 31000 cm^{-1} and the growth of bands at 28000, 22000 and 6500 cm^{-1}. Both the mono-reduced and di-reduced studies were fully reversible.

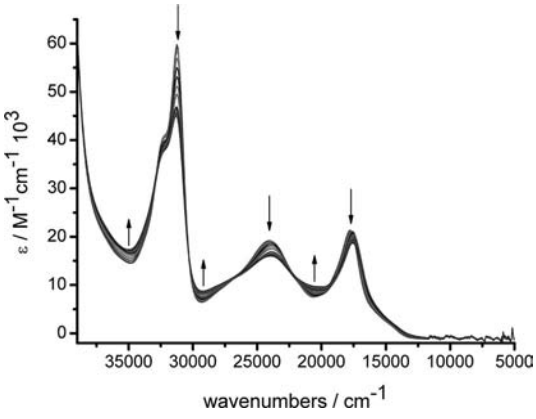

Figure 5. Reductive OTTLE studies in 0.1 M TBABF4/DMF of **1** showing mono-reduced complex, with applied potentials of –1 V (vs. Ag/AgCl).

The room-temperature EPR spectrum of **1** in 0.3 M $TBABF_4$/DCM shows a copper(II) signal, preserved upon cooling to 253 K. The g-factor was 2.09 with a hyperfine splitting value of 75 G, typical of coupling to Cu. Both the mono-oxidised and di-oxidised species show no clear EPR signal; however, the copper(II) signal is once again regenerated upon re-reduction, again demonstrating the reversibility of the oxidation processes. The results from the spectroelectrochemistry study indicate the first oxidation to be Ru-based, and the loss of the EPR signal on oxidation can therefore be attributed to strong exchange coupling of the paramagnetic centres, which would be expected through this bridging moiety.[11]

Unrestricted molecular orbital calculations were carried out on **1** by using hybrid DFT methods with a DMF-polarisable continuum model. Although a crystal structure was not obtained for **1**, the calculated geometry was compared to the bond lengths and angles obtained for Cu(*exo*O_2-cyclam)[9,11] and $[Ru(bpy)_2Cu(exoO_2\text{-cyclam})](NO_3)_2$[11] crystal structures. A comparison of selected parameters (Table S2) shows that the optimised structure has a very good resemblance to that seen in these crystal structures, with most bond lengths and angles in good agreement. The main difference between the two ruthenium complex structures is the angle around the copper atom, with a more asymmetric nature in the calculated structure relative to the XRD structure. This may be due to the presence of the nitrate anions in the XRD structure, and the fact that the calculation is attempting to compensate for the vacant coordination sites by making the centre less planar.

The unpaired electron location was deduced by calculating a spin density, which shows the difference between the α- and β-densities (Figure 6). The unpaired spin density was found to be located on the copper centre, as shown from the positive density in the spin difference map. From the in situ EPR studies it was expected that the location of the unpaired electron would be largely on the copper atom, and this appears to have been recreated by these calculations.

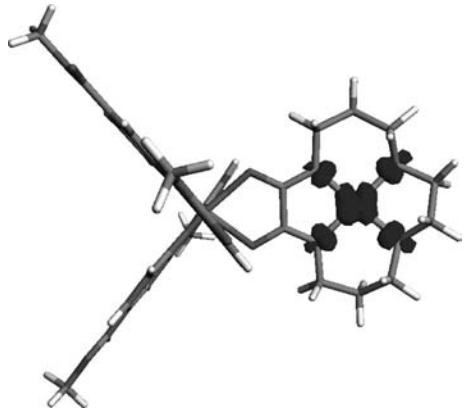

Figure 6. Spin difference isosurface of **1**, showing the difference between the α- and β-densities.

The energies of the HOMO and HOMO-1 orbitals were calculated to be very similar, with only 0.07 eV difference. The HOMO was found to be largely based on the ruthenium centre with a small degree of Cu(*exo*O_2-cyclam) character (Figure S7, Table S3), whereas the HOMO-1 showed significant delocalisation of the orbital over the Cu(*exo*O_2-cyclam). The negligible energy difference calculated between the frontier orbitals based on Ru and Cu indicate the possibility that upon oxidation the dye cation hole may be significantly delocalised over the molecule.

The calculated absorption spectrum of **1** was obtained by TD-DFT using the optimised geometry in a DMF-polarisable continuum model, with 110 singlet transitions calculated in order to simulate the full spectrum. The Gaussian convolution of the calculated transitions shows two absorption bands at 419 and 503 nm (Figure 7, Table S4). The character of the low-energy band was found to consist mostly of HOMO-2 to LUMO excitation. This transition is a mixed Ru/Cu(*exo*O_2-cyclam)-to-bipyridyl charge transfer. The other main contributor to this band is an LLCT (ligand-to-ligand charge transfer) from the Cu(*exo*O_2-cyclam) to the bipyridyl ligand from the HOMO-1 to LUMO+1 orbital. The second band at 419 nm was shown to be largely MLCT (metal-to-ligand charge transfer) in character with a SOMO-to-LUMO+2 transition. Transitions from the SOMO to LUMO were calculated to be at 688 and 605 nm, i.e. of lower energy than the observed bands; however, the transitions also have small oscillator strengths (less than 0.0001), hence the fact that they do not contribute to the calculated spectrum.

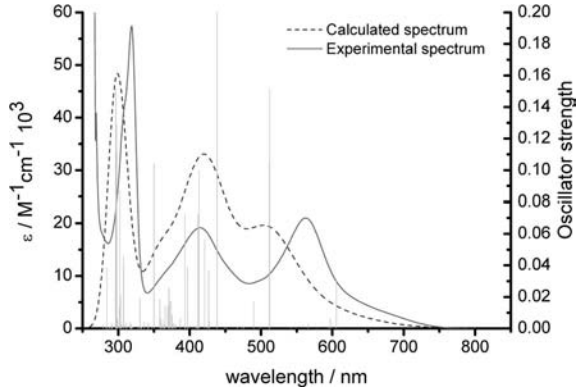

Figure 7. Gaussian convolution of calculated transitions (dashed line), compared to experimental spectrum (solid line), for **1** in DMF, both left axis. The calculated transitions are also shown relative to the oscillator strength (light grey columns), right axis.

Further to this, the fact that there is such a large contribution of the copper(II) to the highest occupied orbitals may be the reason for the observed low emission intensity for this dye series. This may be caused by rapid intramolecular charge-transfer quenching the emission from the MLCT state, or alternatively this may be due to the significant LLCT character resulting in nonradiative decay pathways. It is clearly apparent from these studies that significant communication exists between the Ru and Cu centres, which dominates the electrochemical and spectroscopic behaviour of the complex.

One of the goals of studying a dinuclear dye was to explore the possibility of enhanced charge separation upon photoexcitation at a dye–TiO_2 interface through measuring the time it takes the injected electron in the conduction band to recombine with the oxidised dye. Transient absorption studies were therefore undertaken by using **2** attached to nanocrystalline TiO_2 and covered with various electrolyte solutions. Because of the small magnitude of the conduction-band electron signal (at 1000 nm) obtained with this dye upon photoexcitation, and the fact that there is no clear dye cation absorption band, as shown in the spectroelectrochemical studies, the bleach signal, i.e. the decrease in absorption of the ground state absorption spectrum, was monitored (Figure 8).

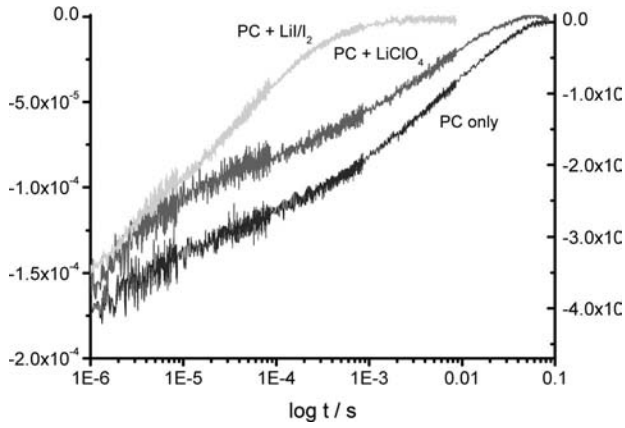

Figure 8. Transient decay traces for **2**–TiO_2 film with propylene carbonate (PC) electrolyte, PC + $LiClO_4$ (both left axis) and PC + LiI/I_2 (right axis). The excitation wavelength was set to 500 nm with the probe at 600 nm.

The study carried out with the dye–TiO_2 film covered with propylene carbonate (PC) showed a recombination half-time of 800 μs; however, with the addition of the $LiClO_4$ this decreased to 100 μs. The purpose of the $LiClO_4$ was to try to increase the electron injection into the conduction band to enable a study of the conduction-band electrons to be made,[32] and whilst the signal at 1000 nm did not significantly increase, the resulting small increase in electrons in the conduction band can result in fewer empty trap sites, leading to electrons recombining with the oxidised dye on a shorter timescale. Interestingly, the recombination half-time was not as long as would have been hoped for this system where secondary electron transfer from the Cu-based ligand might be possible. This also supports the observation of significant contribution of both Cu and Ru centres to the frontier orbitals with strong coupling of the two metal centres. The regeneration dynamics study with the LiI/I_2 electrolyte showed the expected faster decay with a half-time of 20 μs showing that the dye is being regenerated by the redox electrolyte as desired.

Complex **2** was also used to prepare dye-sensitised solar cells by using a variety of cell preparations (Tables S5, S6). In general, a deeply maroon-coloured film was obtained with an absorption spectrum very similar to that seen in solution with a peak at 550 nm (Figure S8) and also a very gradual increase in absorption from 800 nm, showing an increase in absorption relative to N719. The IPCE curve shows a clear correlation to the absorption spectrum of the dye with a peak seen at 545 nm. For the cell that subsequently showed the highest power-conversion efficiency, an IPCE maximum of 31% was observed (Figure 9) and this was achieved with an active area size to 0.3 cm^2, an electrolyte consisting of 0.6 M 1-methyl-3-propylimidazolium iodide (PMII), 0.06 M I_2, 0.5 M NaI, 0.1 M guanid-

inium thiocyanate, 0.5 M *tert*-butyl pyridine (TBP) in 3-methoxypropionitrile, the addition of a compact TiO_2 blocking layer and $TiCl_4$ treatment.

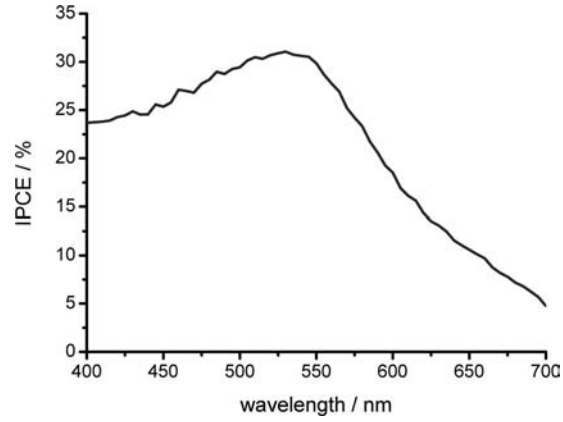

Figure 9. IPCE curve for DSSC sensitised with **2**.

This cell displayed an overall efficiency of 2.55%, with V_{oc} = 608 mV, I_{sc} = 5.84 mA cm^{-2} and *ff* = 0.72 (Figure 10). Under the same conditions a 0.3 cm^2 cell sensitised with N719 gave an efficiency of 6.4%. Although a reasonable efficiency was observed, the lower value compared with N719 suggests some detrimental mechanism is in operation since **2** displays enhanced light harvesting compared with N719 alongside suitable charge-regeneration/recombination dynamics. Possible reasons for the lower performance are explored below.

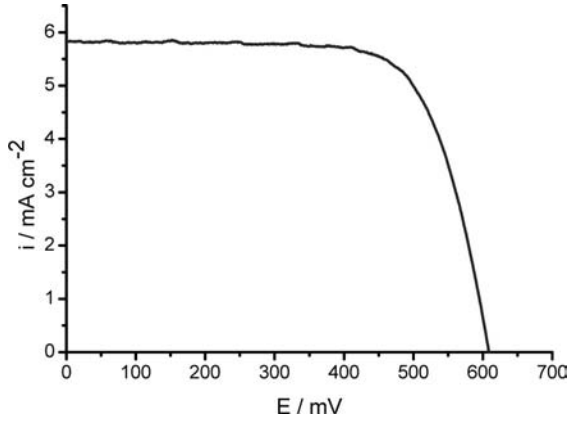

Figure 10. AM1.5 current–voltage characteristics for DSSC sensitised with **2**.

The short-circuit current was seen to increase dramatically upon removing the TBP and guanidinium thiocyanate from the electrolyte of otherwise comparable cells (Tables S5, S6). This increase may indicate that a mismatch between the bipyridyl-based unoccupied orbital of the dye and the conduction band of the TiO_2 was a contributing factor to the low injection efficiency suggested by the transient absorption study. It is thought that the TBP and guanidinium thiocyanate additives reduce the dark current by co-adsorption to the surface of the TiO_2, resulting in effective screening between the TiO_2 and the electrolyte.[33] In addition, removal of TBP and guanidiumium thiocycanate also results in a reduction of the open-circuit voltage, consistent with observations for cells sensitised with N719 whereby these additives cause a negative-shift of the conduction-band edge.[34,35] However, if the energy of the bipyridyl unoccupied orbital is not sufficient for injection, then by removing the additives the conduction-band energy may drop to a level whereby injection is more efficient, hence the increase in photocurrent. As an additional consideration, the global efficiencies of DSSCs sensitised with this dye may be limited by the large degree of fluorescence quenching caused by ET or eT from the $Ru(dcbpy)_2$ moiety to the Cu^{II}.

In addition to these factors, the stability of the dye in the electrolyte solution must be considered. Under prolonged irradiation (AM1.5 light of 1000 W/m^2), cells sensitised with **2** were found to increase in efficiency with time. In addition, the absorption spectrum of the film was observed to show a blueshift of the low-energy absorption maximum. These observations indicate some chemical change of the system upon prolonged exposure to light, particularly in the presence of LiI/I_2 electrolyte. In comparison a prolonged irradiation experiment with a cell sensitised with N719 showed no efficiency variation with time. This suggests the possibility of some ion exchange occurring with the nitrato ligands coordinated to the copper(II) atom displaced perhaps by I^- or I_3^- resulting in the absorption band shift. This is reminiscent of the observed solvent coordination shown in the electrochemical study. Another possibility may be the loss of the copper(II) ligand to the electrolyte. If either of these is the case then the long-term stability of a DSSC sensitised with **2** will be severely affected, although this may not be relevant for noniodide-containing electrolytes.

Conclusions

The synthesis and characterisation of the dyes $[Ru(CO_2R\text{-}bpy)_2\{Cu(exoO_2\text{-}cyclam)\}]$, where R = Et and H, has been successfully achieved, and we have studied for the first time a dinuclear Ru–Cu complex as a sensitiser in a DSSC. The absorption range and molar extinction coefficients of the dyes were significantly increased relative to N719, yielding TiO_2 films sensitised up to 800 nm for the acid derivative (**2**). The electrochemical studies of the dyes showed initial evidence of the redox activity of the Cu-containing ligand being retained in the complex with the presence of two oxidations. Spectroelectrochemical and EPR studies and computational work suggested the first oxidation to be largely Ru-based, with hybrid DFT calculations showing the two highest occupied orbitals to be very close in energy (0.07 eV apart) with one being largely ruthenium- and the other largely copper-based. The DSSCs sensitised with **2** showed a reasonable efficiency of 2.55%. There was, however, evidence for an energy mismatch between the conduction band of the TiO_2 and the bipyridyl-based unoccupied orbital, which appears to be the limiting factor in optimising the efficiency of devices based on this dye. There was also evidence of the dye being unstable in

the presence of the liquid redox electrolyte, which may be caused by the displacement of the nitrate anions around the copper atom or possibly the leaching of the copper(II) ligand into the electrolyte.

Experimental Section

General: Synthesis of $[Ru(decbpy)_2]Cl_2$[36] and [Cu(*exo*O_2-cyclam)][9,10] were carried out according to previously published methods. $RuCl_3 \cdot 3H_2O$ was obtained from Johnson Matthey and all other chemicals were purchased from Aldrich and used as received. Electrochemistry was carried out by using a Pt working electrode, Pt-rod counter electrode and Ag/AgCl reference electrode. All electrochemical experiments were carried out in either DMF or DCM, and the supporting electrolyte used was $TBABF_4$ (0.1 or 0.3 M, respectively). After each experiment, the reference electrode was calibrated against the ferrocene/ferrocenium couple, which was found to be at 0.55 V. The absorption spectra were recorded with a Perkin–Elmer Lambda 9 spectrophotometer controlled by using the UV/Winlab software. Emission spectra were recorded at room temperature with dilute solutions of the dyes in ethanol by using a Fluoromax 2 fluorometer controlled by the ISAMain software. Spectroelectrochemical measurements were recorded at –40 °C with a 0.5 mm Pt-gauze working electrode, Pt-wire counter electrode and an Ag/AgCl reference electrode. Density functional theory calculations of the ester analogues were performed by using the Gaussian 03 program[37] with the starting structure input from the builder program Arguslab. The Becke three-parameters hybrid exchange and Perdew–Wang 1991 correlation functionals (B3PW91) were used.[38,39] For the ruthenium atom a Hay–Wadt VDZ (n+1) ECP was used,[40] and all other atoms were described by 6-31G*. A frequency calculation was performed to ensure the optimised structures were minima on the potential energy surface, verified by the absence of negative values. TD-DFT was performed by using a DMF-polarisable continuum model,[41] with the first 70 singlet transitions calculated. For the preparation of the DSSCs, titanium dioxide paste (Dyesol, DSL-18NR-T) was deposited onto cleaned fluorine-doped tin oxide conductive glass (TEC 8, Pilkington, UK) by doctor-blading. The film was dried at 100 °C for 15 min and then sintered at 450 °C for 30 min to remove the organics and to form a mesoporous film structure. The thickness of the film was about 12 μm. The platinised counter electrode was fabricated according to a previously reported procedure.[42] The cell was completed by sealing the dye-coated TiO_2 electrode and Pt electrode with a thermal-plastic spacer (Surlyn 1702, 25 μm, Solaronix) at 120 °C. The electrolyte [0.6 M 1-methyl-3-propylimidazolium iodide (PMII), 0.06 M I_2, 0.5 M NaI, 0.1 M guanidinium thiocyanate, 0.5 M *tert*-butylpyridine (TBP) in 3-methoxypropionitrile] was introduced into the cell through the two holes, which were drilled in the counter electrode. The holes were subsequently sealed by the thermal plastics (Surlyn 1702, Solaronix) combined with a piece of microscope slide under press. The active area of the cell was 0.3 cm^2. IPCE spectra of the cells were measured with a spectral resolution of 8 nm by using monochromatic light provided by a xenon lamp and monochromator. The incident photon flux was measured with a calibrated Si photodiode. The current/voltage characteristics of the cells were measured under simulated AM1.5 illumination (100 mW cm^{-2}) provided by a solar simulator (1 kW Xe with AM1.5 filter, Müller) calibrated by using a GaAs solar cell. Transient absorption decays were measured with the "flash photolysis" technique. This technique requires that the samples do not absorb or scatter all the incident light. For this reason, instead of complete DSSCs, thin TiO_2 films (about 4 μm) sintered on microscope slides were used. The films were sensitised as described above and covered with a drop of redox-inactive electrolyte (propylene carbonate only or 0.25 M $LiClO_4$ in propylene carbonate) for dye cation-TiO_2(e–) recombination measurements, or with a drop of redox-active electrolyte (0.25 M LiI, 0.05 M I_2 in propylene carbonate) for the dye regeneration measurements. The samples were excited with a dye laser (Photon Technology International Inc., GL-301) pumped by a nitrogen laser (Photon Technology International Inc., GL-3300). The excitation wavelength was 500 nm, the pulse width was 800 ps, the fluence was about 50 μJ cm^{-2}, and the repetition frequency was 1 Hz. A 100 W tungsten-halogen lamp (Bentham, IL1) with a stabilised power supply (Bentham, 605) was used as a probe light source. The probe light passing through the sample was detected with a silicon photodiode (Hamamatsu Photonics, S1722-01). The signal from the photodiode was pre-amplified and sent to the main amplification system with an electronic band-pass filter to improve signal-to-noise ratio (Costronics Electronics). The amplified signal was collected with a digital oscilloscope (Tektronix, TDS 220), which was synchronised with a trigger signal of the laser pulse from a photodiode (Thorlabs Inc., DET210). To reduce stray light, scattered light and emission from the sample, two monochromators and appropriate optical cut-off filters were placed before and after the sample. Owing to the amplification and noise-reduction system, the detectable change of absorbance was as small as 10^{-5} to 10^{-6}.

Cu(*exo*O_2-cyclam): $C_{10}H_{18}CuN_4O_2$ (289.82): calcd. C 41.44, H 6.26, N 19.33; found C 41.58, H 6.61, N 18.75.

[Ru(decbpy)$_2${Cu(*exo*O_2-cyclam)}](NO$_3$)$_2$ (1): $[Ru(decbpy)_2]Cl_2$ (100 mg, 0.129 mmol) was dissolved in methanol (10 mL), and silver nitrate (44 mg, 0.26 mmol) in water (1 mL) was added. The mixture was refluxed in the dark under N_2 for 1 h. The resultant precipitate (silver chloride) was removed by centrifugation. To the solution [Cu(*exo*O_2-cyclam)] (38 mg, 0.129 mmol) was added as a solid and the mixture stirred under N_2 and in the dark overnight. The solution was filtered and the filtrate concentrated in a rotary evaporator, diethyl ether was layered on top and the flask placed in the refridgerator. The resulting maroon precipitate was collected by filtration. The crude product was furthered purified on a Sephadex LH-20 column by using methanol as the eluent, collecting the main purple band. Yield: 98 mg (68%). $C_{42}H_{54}CuN_{10}O_{18}Ru$ (1151.56): calcd. C 43.81, H 4.73, N 12.16; found C 43.50, H 4.05, N 11.81. MS (FAB+): m/z = 1054 [M – NO_3]$^+$, 990 [M – 2 NO_3 – H]$^+$, 702 [Ru(decbpy)$_2$]$^+$.

[Ru(dcbpy)$_2${Cu(*exo*O_2-cyclam)}](NO$_3$)$_2$ (2): $[Ru(decbpy)_2]Cl_2$ (100 mg, 0.129 mmol) was dissolved in methanol (10 mL), and silver nitrate (44 mg, 0.26 mmol) in water (1 mL) was added. The mixture was refluxed in the dark under N_2 for 1 h. The resultant precipitate (silver chloride) was removed by centrifugation. 0.1 M KOH (3 mL) was added and the solution stirred for 15 min. To this solution [Cu(*exo*O_2-cyclam)] (38 mg, 0.129 mmol) was added as a solid and the mixture stirred under N_2 and in the dark overnight. The product was precipitated by the addition of 1 M HNO_3 (2 mL), the resulting maroon precipitate was further purified on a Sephadex LH-20 column by using water as the eluent, collecting the main purple band. Yield: 19 mg (16%). $C_{34}H_{44}CuN_{10}O_{22}Ru$ (1109.39): calcd. C 36.81, H 3.99, N 12.63; found C 35.66, H 3.09, N 12.72. MS (ESI–): m/z = 439 [M – 2 NO_3]$^{2+}$.

Supporting Information (see footnote on the first page of this article): Cyclic voltammograms of **1** in DMF and DCM; excitation and emission spectra for **1**; spectroelectrochemical (OTTLE) studies of

1; hybrid DFT computational results for **1**. UV/Vis spectrum of **2** on TiO_2; I–V behaviour of solar cells based on **2**.

Acknowledgments

The Excitonic Solar Cell Consortium (EPSRC) are gratefully acknowledged for funding. Johnson Matthey are gratefully acknowledged for the loan of $RuCl_3 \cdot 3H_2O$. We have made use of the resources provided by the EaStCHEM Research Computing Facility (http://www.eastchem.ac.uk/rcf), partially supported by the eDIKT initiative (http://www.edikt.org.).

[1] a) N. Robertson, *Angew. Chem. Int. Ed.* **2006**, *45*, 2338; b) Md. K. Nazeeruddin, C. Klein, P. Liska, M. Grätzel, *Coord. Chem. Rev.* **2005**, *249*, 1460.
[2] Md. K. Nazeeruddin, P. Liska, J. Moser, N. Vlachopoulos, M. Grätzel, *Helv. Chim. Acta* **1990**, *73*, 1788–1803.
[3] a) C. A. Bignozzi, J. R. Schoonover, F. Scandola, *Prog. Inorg. Chem.* **1997**, *44*, 1–95; b) C. A. Bignozzi, R. A. Argazzi, C. J. Kleverlaan, *Chem. Soc. Rev.* **2000**, *29*, 87–96.
[4] A. C. Lees, C. J. Kleverlaan, C. A. Bignozzi, J. G. Vos, *Inorg. Chem.* **2001**, *40*, 5343–5349.
[5] B. Gholamkhass, K. Koike, N. Negishi, H. Hori, T. Sano, K. Takeuchi, *Inorg. Chem.* **2003**, *42*, 2919–2932.
[6] C. Chiorboli, S. Fracasso, F. Scandola, S. Campagna, S. Serroni, R. Konduri, F. M. Macdonnell, *Chem. Commun.* **2003**, 1658–1659.
[7] Md. K. Nazeeruddin, M. Grätzel, *Comput. Coord. Chem. II* **2003**, *9*, 719–758.
[8] Y. Xu, G. Eilers, M. Borgström, J. Pan, M. Abrahamsson, A. Magnuson, R. Lomoth, J. Bergquist, T. Polívka, L. Sun, V. Sundström, S. Styring, L. Hammarström, B. Åkermark, *Chem. Eur. J.* **2005**, *11*, 7305–7314.
[9] L. Cronin, A. R. Mount, S. Parsons, N. Robertson, *J. Chem. Soc., Dalton Trans.* **1999**, 1925–1927.
[10] L. Cronin, P. A. McGregor, S. Parsons, S. Teat, R. O. Gould, V. A. White, N. J. Long, N. Robertson, *Inorg. Chem.* **2004**, *43*, 8023–8029.
[11] V. A. White, R. D. L. Johnstone, K. L. McCall, N. J. Long, A. M. Z. Slawin, N. Robertson, *Dalton Trans.* **2007**, 2942–2948.
[12] H.-Z. Kou, B. C. Zhou, S. Gao, R.-J. Wang, *Angew. Chem. Int. Ed.* **2003**, *42*, 3288–3291.
[13] J.-K. Tang, Y. Ou-Yang, H.-B. Zhou, Y.-Z. Li, D.-Z. Liao, Z. H. Jiang, S.-P. Yan, P. Cheng, *Cryst. Growth Des.* **2005**, *5*, 813–819.
[14] J.-K. Tang, S.-F. Si, L.-Y. Wang, D.-Z. Liao, Z.-H. Jiang, S.-P. Yan, P. Cheng, X. Liu, *Inorg. Chem. Commun.* **2002**, *5*, 1012–1015.
[15] J.-K. Tang, S.-F. Si, E.-Q. Gao, D.-Z. Liao, Z.-H. Jiang, S.-P. Yan, *Inorg. Chim. Acta* **2002**, *332*, 146–152.
[16] J.-K. Tang, L.-Y. Wang, L. Zhang, E.-Q. Gao, D.-Z. Liao, Z.-H. Jiang, S.-P. Yan, P. Cheng, *J. Chem. Soc., Dalton Trans.* **2002**, 1607–1612.
[17] J.-K. Tang, Y.-Z. Li, Q.-L. Wang, E.-Q. Gao, D.-Z. Liao, Z.-H. Jiang, S.-P. Yan, P. Cheng, L.-F. Wang, G.-L. Wang, *Inorg. Chem.* **2002**, *41*, 2188–2192.
[18] H.-Z. Kou, B. C. Zhou, R.-J. Wang, *Inorg. Chem.* **2003**, *42*, 7658–7665.
[19] M. Osawa, H. Sonoki, M. Hoshino, Y. Wakatsuki, *Chem. Lett.* **1998**, 1081–1082.
[20] B. Geißer, R. Alsfasser, *Eur. J. Inorg. Chem.* **1998**, 957–963.
[21] B. Geißer, R. Alsfasser, *Dalton Trans.* **2003**, 612–618.
[22] N. Onozawa-Komatsuzaki, R. Katoh, Y. Himeda, H. Sugihara, H. Arakawa, K. Kasuga, *Bull. Chem. Soc. Jpn.* **2003**, *76*, 977–984.
[23] D. Bruce, M. M. Richter, *Analyst* **2002**, *127*, 1492–1494.
[24] A. Hazell, R. Hazell, C. J. McKenzie, L. P. Nielsen, *Dalton Trans.* **2003**, 2203–2208.
[25] S. C. Rawle, P. Moore, N. W. Alcock, *J. Chem. Soc., Chem. Commun.* **1992**, 684–687.
[26] F. Bolletta, I. Costa, L. Fabbrizzi, M. Licchelli, M. Montalti, P. Pallavicini, L. Prodi, N. Zaccheroni, *J. Chem. Soc., Dalton Trans.* **1999**, 1381–1385.
[27] K. L. McCall, J. R. Jennings, H. Wang, A. Morandeira, L. M. Peter, J. R. Durrant, L. J. Yellowlees, J. D. Woollins, N. Robertson, *J. Photochem. Photobiol. A: Chem.* **2009**, *202*, 196–204.
[28] Md. K. Nazeeruddin, A. Kay, I. Rodicio, R. Humphry-Baker, E. Müller, P. Liska, N. Vlachopoulos, M. Grätzel, *J. Am. Chem. Soc.* **1993**, *115*, 6382–6390.
[29] Y. Takahashi, H. Arakawa, H. Sugihara, K. Hara, A. Islam, R. Katoh, Y. Tachibana, M. Yanagida, *Inorg. Chim. Acta* **2000**, *310*, 169–174.
[30] a) H. G. Agrell, J. Lindgren, A. Hagfeldt, *Solar Energy* **2003**, *75*, 169; b) H. G. Agrell, J. Lindgren, A. Hagfeldt, *J. Photochem. Photobiol. A: Chem.* **2004**, *164*, 23.
[31] K. L. McCall, A. Morandeira, J. R. Durrant, L. J. Yellowlees, N. Robertson, *Dalton Trans.* **2010**, *39*, 4138.
[32] A. Staniszewski, S. Ardo, Y. Sun, F. N. Castellano, G. J. Meyer, *J. Am. Chem. Soc.* **2008**, *130*, 11586.
[33] M. Grätzel, *J. Photochem. Photobiol. A: Chem.* **2004**, *164*, 3–14.
[34] X. Yin, H. Zhao, L. Chen, W. Tan, J. Zhang, Y. Weng, Z. Shuai, X. Xiao, X. Zhou, X. Li, Y. Lin, *Surf. Interface Anal.* **2007**, *39*, 809–816.
[35] H. Kusama, H. Orita, H. Sugihara, *Sol. J. Energ. Mater. Sol. Cells* **2008**, *92*, 84–87.
[36] G. Wolfbauer, A. M. Bond, D. R. MacFarlane, *Inorg. Chem.* **1999**, *38*, 3836–3846.
[37] M. J. Frisch, G. W. Trucks, H. B. Schlegel, G. E. Scuseria, M. A. Robb, J. R. Cheeseman, J. A. Montgomery Jr., T. Vreven, K. N. Kudin, J. C. Burant, J. M. Millam, S. S. Iyengar, J. Tomasi, V. Barone, B. Mennucci, M. Cossi, G. Scalmani, N. Rega, G. A. Petersson, H. Nakatsuji, M. Hada, M. Ehara, K. Toyota, R. Fukuda, J. Hasegawa, M. Ishida, T. Nakajima, Y. Honda, O. Kitao, H. Nakai, M. Klene, X. Li, J. E. Knox, H. P. Hratchian, J. B. Cross, V. Bakken, C. Adamo, J. Jaramillo, R. Gomperts, R. E. Stratmann, O. Yazyev, A. J. Austin, R. Cammi, C. Pomelli, J. W. Ochterski, P. Y. Ayala, K. Morokuma, G. A. Voth, P. Salvador, J. J. Dannenberg, V. G. Zakrzewski, S. Dapprich, A. D. Daniels, M. C. Strain, O. Farkas, D. K. Malick, A. D. Rabuck, K. Raghavachari, J. B. Foresman, J. V. Ortiz, Q. Cui, A. G. Baboul, S. Clifford, J. Cioslowski, B. B. Stefanov, G. Liu, A. Liashenko, P. Piskorz, I. Komaromi, R. L. Martin, D. J. Fox, T. Keith, M. A. Al-Laham, C. Y. Peng, A. Nanayakkara, M. Challacombe, P. M. W. Gill, B. Johnson, W. Chen, M. W. Wong, C. Gonzalez, J. A. Pople, *Gaussian 03*, Revision C.02, Gaussian, Inc., Wallingford, CT, **2004**.
[38] J. P. Perdew, J. A. Chevary, S. H. Vosko, K. A. Jackson, M. R. Pederson, D. J. Singh, C. Fiolhais, *Phys. Rev. B* **1993**, *48*, 4978–4978.
[39] J. P. Perdew, K. Burke, Y. Wang, *Phys. Rev. B* **1996**, *54*, 16533–16539.
[40] P. J. Hay, W. R. Wadt, *J. Chem. Phys.* **1985**, *82*, 299–310.
[41] E. S. Boes, P. R. Livotto, H. Stassen, *Chem. Phys.* **2006**, *331*, 142–158.
[42] N. Papageorgiou, W. F. Maier, M. Grätzel, *J. Electrochem. Soc.* **1997**, *144*, 876–884.

Received: September 30, 2010
Published Online: December 27, 2010

